



TITLE:

PDK2 leads to cisplatin resistance through suppression of mitochondrial function in ovarian clear cell carcinoma

AUTHOR(S):

Kitamura, Sachiko; Yamaguchi, Ken; Murakami, Ryusuke; Furutake, Yoko; Higasa, Koichiro; Abiko, Kaoru; Hamanishi, Junzo; Baba, Tsukasa; Matsumura, Noriomi; Mandai, Masaki

CITATION:

Kitamura, Sachiko ...[et al]. PDK2 leads to cisplatin resistance through suppression of mitochondrial function in ovarian clear cell carcinoma. *Cancer Science* 2021, 112(11): 4627-4640

ISSUE DATE:

2021-11




URL:

<http://hdl.handle.net/2433/277455>

RIGHT:

© 2021 The Authors. *Cancer Science* published by John Wiley & Sons Australia, Ltd on behalf of Japanese Cancer Association.; This is an open access article under the terms of the Creative Commons Attribution-NonCommercial-NoDerivs License, which permits use and distribution in any medium, provided the original work is properly cited, the use is non-commercial and no modifications or adaptations are made.

PDK2 leads to cisplatin resistance through suppression of mitochondrial function in ovarian clear cell carcinoma

Sachiko Kitamura¹ | Ken Yamaguchi¹  | Ryusuke Murakami¹  | Yoko Furutake¹ | Koichiro Higasa² | Kaoru Abiko¹ | Junzo Hamanishi¹  | Tsukasa Baba³ | Noriomi Matsumura⁴ | Masaki Mandai¹

¹Department of Gynecology and Obstetrics, Graduate School of Medicine, Kyoto University, Kyoto, Japan

²Department of Genome Analysis, Institute of Biomedical Science, Kansai Medical University, Hirakata, Japan

³Department of Obstetrics and Gynecology, Iwate Medical University School of Medicine, Morioka, Japan

⁴Department of Obstetrics and Gynecology, Faculty of Medicine, Kindai University, Osaka-Sayama, Japan

Correspondence

Ken Yamaguchi, 54 Kawahara-cho, Shogoin, Sakyo-ku, Kyoto 606-8507, Japan.
Email: soulken@kuhp.kyoto-u.ac.jp

Funding information

Grant-in-Aid for Scientific Research (KAKENHI), Grant/Award Number: 20378772

Abstract

Ovarian clear cell carcinoma (CCC) exhibits an association with endometriosis, resistance to oxidative stress, and poor prognosis owing to its resistance to conventional platinum-based chemotherapy. A greater understanding of the molecular characteristics and pathogenesis of ovarian cancer subtypes may facilitate the development of targeted therapeutic strategies, although the mechanism of drug resistance in ovarian CCC has yet to be determined. In this study, we assessed exome sequencing data to identify new therapeutic targets of mitochondrial function in ovarian CCC because of the central role of mitochondria in redox homeostasis. Copy number analyses revealed that chromosome 17q21-24 (chr.17q21-24) amplification was associated with recurrence in ovarian CCC. Cell viability assays identified an association between cisplatin resistance and chr.17q21-24 amplification, and mitochondrion-related genes were enriched in patients with chr.17q21-24 amplification. Patients with high expression of pyruvate dehydrogenase kinase 2 (PDK2) had a worse prognosis than those with low PDK2 expression. Furthermore, inhibition of PDK2 synergistically enhanced cisplatin sensitivity by activating the electron transport chain and by increasing the production of mitochondrial reactive oxygen species. Mouse xenograft models showed that inhibition of PDK2 with cisplatin inhibited tumor growth. This evidence suggests that targeting mitochondrial metabolism and redox homeostasis is an attractive therapeutic strategy for improving drug sensitivity in ovarian CCC.

Abbreviations: ARID1A, AT-rich interaction domain 1A; ATP, adenosine triphosphate; CCC, clear cell carcinoma; CDDP, cisplatin; CGH, comparative genomic hybridization; CNV, copy number variant; CPT11, camptothecin; CTNNB1, catenin beta 1; DAVID, database for annotation, visualization and integrated discovery; DCA, sodium dichloroacetate; DXR, doxorubicin; ETC, respiratory electron transport chain; FADH₂, dihydro-flavin adenine dinucleotide; FDR, false discovery rate; GBE1, glycogen branching enzyme; GEM, gemcitabine; GSH, L-glutathione reduced; GYS1, glycogen synthase; H₂O₂, hydrogen peroxide; HGSC, high-grade serous carcinoma; HIF1A, hypoxia-inducible factor-1 α ; HNF1B, HNF1 homeobox B; HR, hazard ratio; IC50, half maximal inhibitory concentration; IHC, immunohistochemistry; MDM2, MDM2 proto-oncogene; NAC, N-acetyl-L-cysteine; NADH, nicotinamide adenine dinucleotide hydrogen; OCR, oxygen consumption rate; OS, overall survival; OXPHOS, oxidative phosphorylation; PDC, pyruvate dehydrogenase complex; PDH, pyruvate dehydrogenase; PDHE1, pyruvate dehydrogenase E1 component subunit; PDK, pyruvate dehydrogenase kinase; PDK2, pyruvate dehydrogenase kinase 2; PFS, progression-free survival; PIK3CA, phosphatidylinositol-4,5-bisphosphate 3-kinase catalytic subunit alpha; PLD, doxorubicin hydrochloride liposome; PPGM1, phosphoglucomutase 1; PPM1D, protein phosphatase, Mg²⁺/Mn²⁺ dependent 1D; PPP1R3C, protein phosphatase 1 regulatory subunit 3C; PTEN, phosphatase, tensin homolog; PTX, paclitaxel; PYGL, glycogen phosphorylase; ROS, reactive oxygen species; SLC31A1, solute carrier family 31 member 1; SLC3A1, solute carrier family 3 member 1; TALEN, transcription activator-like effector nuclease; TCA, tricarboxylic acid; UGP2, UDP-glucose pyrophosphorylase.

This is an open access article under the terms of the Creative Commons Attribution-NonCommercial-NoDerivs License, which permits use and distribution in any medium, provided the original work is properly cited, the use is non-commercial and no modifications or adaptations are made.

© 2021 The Authors. *Cancer Science* published by John Wiley & Sons Australia, Ltd on behalf of Japanese Cancer Association.

KEYWORDS

chemoresistance, clear cell carcinoma, mitochondria, ovarian cancer, pyruvate dehydrogenase kinase isoform 2

1 | INTRODUCTION

Ovarian cancer has the worst clinical behavior among gynecologic malignancies.¹ Considerable heterogeneity exists within and between well-established ovarian cancer subtypes and their drug sensitivities.² Four distinct nomenclatures are used to classify ovarian cancer based on morphological criteria: high-grade serous carcinoma (HGSC), mucinous carcinoma, endometrioid carcinoma, and clear cell carcinoma (CCC).² CCC is the second most common subtype after HGSC and accounts for 25% of all cases of ovarian cancer in Japan.³ Ovarian CCC has a poor prognosis owing to its resistance to conventional platinum-based chemotherapy at advanced stages.³ Therefore, specific therapeutic strategies for overcoming chemoresistance are urgently needed for ovarian CCC. Ovarian CCC-specific somatic mutations have been reported in AT-rich interaction domain 1A (*ARID1A*), phosphatidylinositol-4,5-bisphosphate 3-kinase catalytic subunit alpha (*PIK3CA*), phosphatase, tensin homolog (*PTEN*), and catenin beta 1 (*CTNNB1*).⁴ However, the pathway alterations responsible for chemoresistance in CCC have not been identified. Simply targeting these genes does not lead to effective therapy, indicating the underlying genomic and epigenomic complexity of ovarian CCC.⁵ Elucidation of the biological mechanisms essential for the survival of cancer cells is necessary to identify useful treatments for ovarian CCC.

We previously reported that oxidative stress in an iron-rich environment induced accumulation of gene mutations and induced the characteristic gene expression profile (OCCC signature) for ovarian CCC.^{6,7} In the OCCC signature, we focused on HNF1 homeobox B (*HNF1B*) in terms of glucose metabolism, redox homeostasis and cisplatin resistance. HNF1B inhibits glucose influx into the tricarboxylic acid (TCA) cycle and induces solute carrier family 3 member 1 (*SLC3A1*) expression, which decreases intracellular reactive oxygen species (ROS) activity by promoting glutathione synthesis in ovarian CCC cell lines.⁸ These findings suggest that HNF1B, which is induced in a persistent iron-rich oxidative stress environment, plays a crucial role in glucose metabolism and controlling ROS production in ovarian CCC, suggesting that one of the mechanisms of cisplatin resistance in ovarian CCC is maintenance of redox homeostasis.

In living organisms, ROS are generated through the respiratory electron transport chain (ETC) in mitochondria, a process called oxidative phosphorylation (OXPHOS).⁹ Either ETC overload or disruption at any of these locations may lead to blockage of electrons upstream, which allows the electrons to react with oxygen to produce superoxide.^{10,11} Thus, mitochondrial ETC plays the main role in ROS production. The electrons are provided as nicotinamide adenine dinucleotide hydrogen (NADH) and dihydroflavin adenine

dinucleotide (FADH₂) from the TCA cycle into the OXPHOS pathway. That is, the regulation of the flux into the TCA cycle can change the production of ROS in the mitochondrial ETC, thereby reflecting the changes in NADH and FADH₂ production. One of the enzymes controlling flux into the TCA cycle is pyruvate dehydrogenase kinase (PDK). PDK suppresses the conversion of pyruvic acid to acetyl coenzyme A, which enters the TCA cycle in mitochondria by inhibiting pyruvate dehydrogenase (PDH) through phosphorylation of Ser293 on the E1 α subunit of PDH (PDHE1-alpha).^{12,13} However, the role of PDK in chemoresistance has not yet been elucidated in ovarian CCC.

In this study, we present a new potential therapeutic target for overcoming chemoresistance by targeting mitochondrial metabolism and disrupting redox homeostasis through pyruvate dehydrogenase kinase 2 (PDK2) based on the exploration of the essential biological mechanisms in ovarian CCC.

2 | MATERIALS AND METHODS

The details are described in the Supporting Information. This study was approved by the Kyoto University Graduate School and Faculty of Medicine Ethics Committee.

2.1 | Whole-exome sequencing

Genomic DNA was extracted from 13 ovarian CCC cell lines using QIAamp DNA Mini Kits (Qiagen) following the manufacturer's protocols. The quality of the DNA was assessed for purity and concentration using a NanoDrop spectrophotometer (Thermo Fisher Scientific KK) according to the manufacturer's quality control methods. Whole-exome sequencing was performed using Agilent SureSelect Human All Exon V5 (Agilent Technologies).

2.2 | Copy number analysis

Differential coverages between tumor and normal tissues from 39 patients were calculated with a custom script and used for copy number analysis. For samples for which corresponding normal tissues were not available, the average coverage of the exome sequencing data from normal tissues of the other 16 patients was used as the coverage of normal tissue. For the 13 ovarian CCC cell lines, the average coverage of the cell lines was used as the same common reference. The data are available at the repository website of

the Human Genetic Variation Database (<https://www.hgvd.genome.med.kyoto-u.ac.jp/repository.html>).

2.3 | Gene expression microarray analysis

Gene expression microarray data from the GSE39204¹⁴ and GSE55512¹⁵ datasets were used for gene expression analysis. Gene expression microarray datasets for ovarian cancer cell lines that included CCC and serous subtypes (GSE29175)⁷ were obtained from the Gene Expression Omnibus website.

2.4 | Immunohistochemical analysis of clinical ovarian clear cell carcinoma

Immunostaining of PDK2 was evaluated using the immunohistochemistry (IHC) score. The IHC score is defined by the staining intensity score multiplied by the percentage of tumor cells with staining. The staining intensity was classified as follows: 0, negative; 1, weak; 2, moderate; and 3, strong expression (see Figure 2A). The stained area ranged from 0% to 100% in increments of 10%. Cases were divided into high and low PDK2 expression groups according to the IHC score. The high-PDK2 group had IHC scores greater than the median, and the low-PDK2 group had IHC scores lower than the median.

2.5 | Cell viability assay

Thirteen ovarian CCC cell lines (RMG1, RMG2, RMG5, KOC5c, KOC7c, JHOC5, JHOC7, JHOC8, JHOC9, TOV21G, OVTOKO, OVISE, and TAYA cell lines) were described in detail in our previous paper.⁷ After exposure to the chemotherapeutic agents for 72 hours, cell viability was assessed using a WST-8 assay with Cell Count Reagent SF (NACALAI TESQUE). The chemotherapeutic agents used were as follows: cis-diammineplatinum(II) dichloride (cisplatin [CDDP], Sigma-Aldrich Japan), camptothecin (CPT11, Sigma-Aldrich Japan), paclitaxel (PTX, Bristol-Myers Squibb KK), gemcitabine (GEM, Eli Lilly Japan KK), doxorubicin (DXR, Sigma-Aldrich Japan), doxorubicin hydrochloride liposome (PLD, Janssen Pharmaceutical KK), sodium dichloroacetate (DCA, Sigma-Aldrich Japan), N-acetyl-L-cysteine (NAC, Sigma-Aldrich Japan), and L-glutathione reduced (GSH, Sigma-Aldrich Japan).

2.6 | Stable knockdown using shRNA and overexpression of pyruvate dehydrogenase kinase 2

RMG1 knockdown cells were generated by lentiviral transfection using two different GIPZ lentiviral shRNA and a nonsilencing control RNA. PDK2 overexpression in RMG5 cells, which showed low expression of PDK2, was generated by lentiviral transfection using a

Precision LentiORF (Horizon Discovery Group). We used blasticidin for selection and confirmed the overexpression of PDK2 by RT-PCR and western blotting.

2.7 | Mitochondrial reactive oxygen species production and mitochondrial membrane potential

After treatment with the drugs for 24 hours, mitochondrial ROS generation was detected using the mitoSOX Red mitochondrial superoxide indicator (Thermo Fisher Scientific KK). The mitochondrial membrane potential was detected in cells that were incubated with MitoTracker RedCM-H2Xros (Thermo Fisher Scientific KK).

2.8 | Measurement of the oxygen consumption rate

Mitochondrial stress tests were performed with an Agilent Seahorse XF96 Extracellular Flux Analyzer (Agilent Technologies) following the manufacturer's instructions. The parameters were calculated using Wave software (Agilent Technologies).

2.9 | Mouse xenograft models

Tumor cells were injected subcutaneously into the flanks of 6-week-old athymic ICR/nu female mice (5×10^6 cells). Tumors were measured using a caliper, and tumor volume was calculated as follows: $(\text{length} \times \text{width}^2)/2$. Mice were randomized into four groups. Experimental group 1 included RMG1-shcontrol treated with mock, RMG1-shcontrol treated with CDDP, RMG1-shPDK2 treated with mock, and RMG1-shPDK2 treated with CDDP. Experimental group 2 included RMG1-WT treated with mock, RMG1-WT treated with CDDP, RMG1-WT treated with DCA, and RMG1-WT treated with CDDP and DCA. The animal study was performed according to protocols approved by the Institutional Animal Care and Use Committee of Kyoto University.

3 | RESULTS

3.1 | Chromosome 17q21-24 amplification is associated with recurrence, resistance to cisplatin, and mitochondria in ovarian clear cell carcinoma

Samroc analysis between patients with recurrence and those without recurrence identified that amplification on chromosome 17q21-24 (chr.17q21-24) was significantly associated with a poor prognosis in terms of progression-free survival (PFS) in 37 exome datasets (false discovery rate [FDR] $q < 0.01$) (Figure 1A-upper). Using external validation datasets of comparative genomic hybridization (CGH) arrays and 111 CCC samples, we also identified chr.17q21-24 amplification in patients with recurrence (GSE58342, Figure 1A-lower).

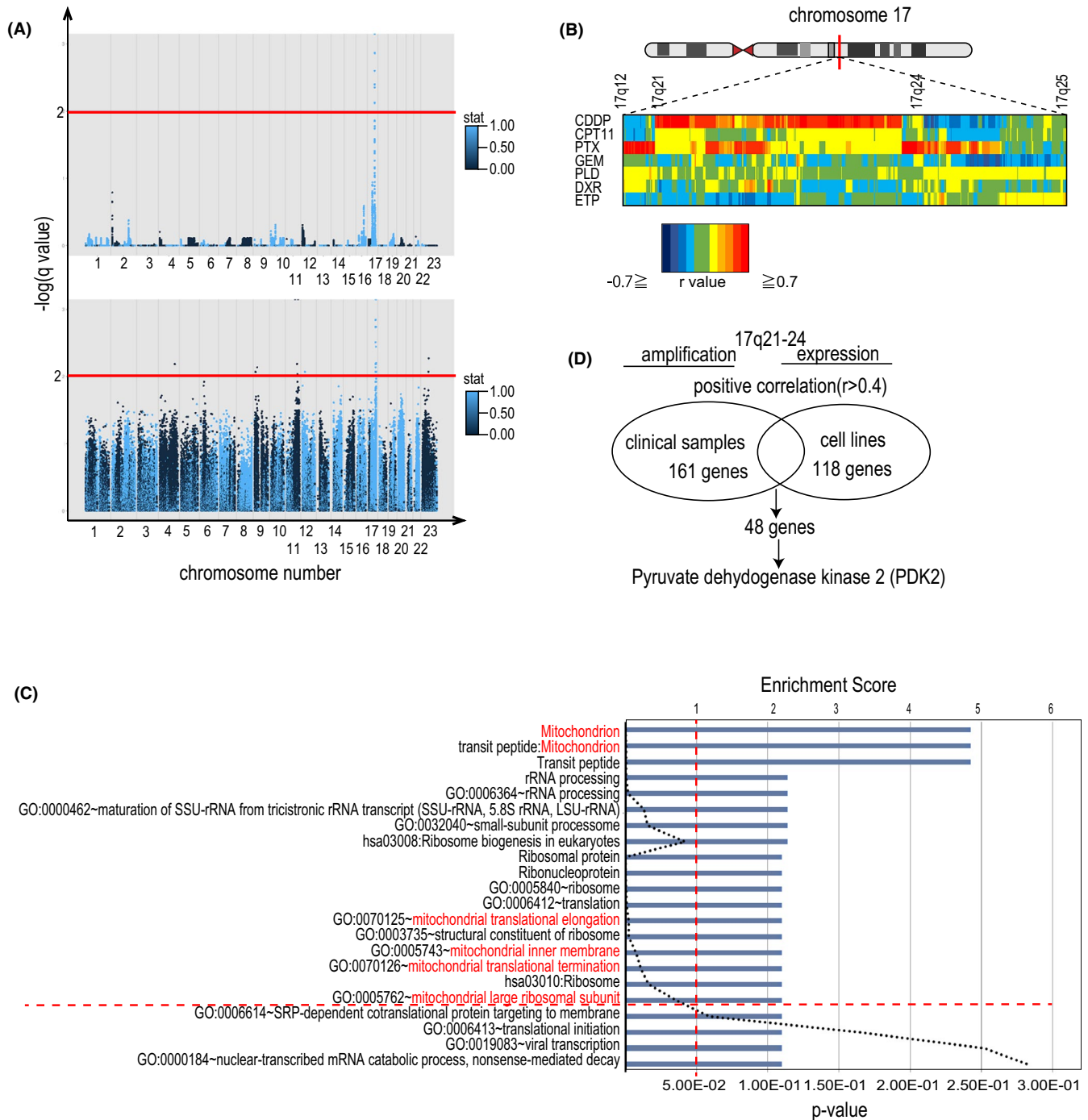


FIGURE 1 Chromosome 17q21-24 amplification is associated with recurrence, resistance to cisplatin, and mitochondria in ovarian clear cell carcinoma (CCC). A, Copy number variants from the whole-exome sequencing of 37 ovarian CCC patients (upper graph) and array comparative genomic hybridization (CGH) of 111 patients (GSE 58342, lower) showed the association between chr17q21-24 and cancer recurrence. The lighter blue color indicates the amplified loci within the recurrent group (n = 12) or deleted loci within the nonrecurrent (n = 25) group. The darker blue colors indicate the amplified loci within the nonrecurrent group or deleted loci within the recurrent group. The plots above the red line indicate a significance level of less than .05 for FDR q-values. B, Amplification on chr17q21-24 was positively correlated with the IC50 values of cisplatin (CDDP). Heat map representing values of Pearson's correlation coefficients (r) between the amplification of genes located on chr17q12-25 and the IC50 values of the six anticancer drugs (CDDP; cisplatin, CPT11; camptothecin II; PTX, paclitaxel; GEM, gemcitabine, PLD, doxorubicin hydrochloride (pegylated liposomal); DXR, doxorubicin; and ETP, etoposide). C, The term associated with mitochondria (highlighted in red) was enriched in patients with 17q amplification. Bar and dotted line chart representing enrichment scores and P-values, respectively, calculated by functional annotation analysis (DAVID 6.8, https://david.ncicrf.gov/home.jsp) of the genes upregulated in the patients with clinical 17q amplification. D, Schema of identifying the pyruvate dehydrogenase kinase 2 (PDK2) gene from the overlapping 48 genes in 18 clinical samples (GSE 39204 and GSE 5512) and 13 cell lines (GSE 29175). These genes have a positive correlation ($r > .4$) between expression and amplification within chr17q21-24.

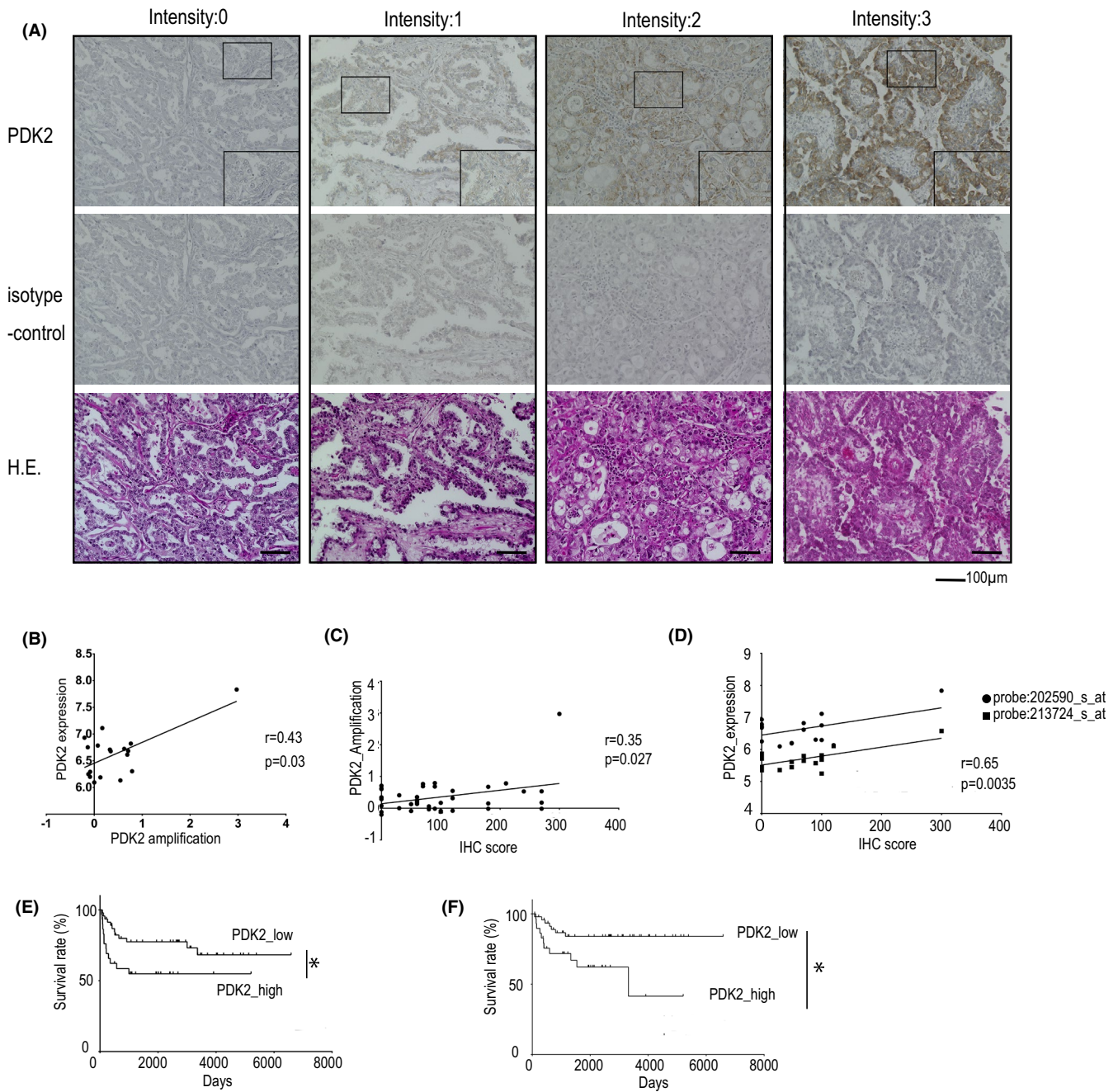


FIGURE 2 High pyruvate dehydrogenase kinase 2 (PDK2) expression is associated with poor prognosis in 76 ovarian clear cell carcinoma (CCC) patients. A, Representative images of immunostaining for PDK2 and H&E of its isotype control (magnification: $\times 20$, $\times 30$ [indicated by the small box]). B-D, Correlation analysis of PDK2 amplification and mRNA expression in 18 clinical samples (GSE 39204 and GSE 5512) (B), immunohistochemistry (IHC) score and PDK2 amplification in 39 clinical samples (C), and IHC score and PDK2 mRNA expression (two types of probes were used to identify *PDK2*) in 18 clinical samples (GSE 39204 and GSE 5512) (D). The r values represent Pearson's correlation coefficient. E and F, Kaplan-Meier curve according to PDK2 expression (46 samples of PDK2 high and 30 samples of PDK2 low) representing OS (E) and PFS (F). (* $P < .05$, Mantel-Cox Log-rank test)

To investigate the relationship between chr.17q21-24 amplification and drug resistance, the correlation between the copy number variant (CNV) values of the genes on 17q21-24 and the half maximal inhibitory concentration (IC50) values of six anticancer agents was assessed (Table S1). The values of CNV on chr.17q21-24 were positively correlated with the IC50 values of cisplatin ($r > .7$) but not with other anticancer drugs in the 13 ovarian CCC cell lines,

suggesting that chr.17q21-24 is associated with resistance to cisplatin (Figure 1B). Other regions also showed positive correlations between the CNV and the IC50 value of cisplatin (Figure S1), but we focused on chr.17q21-24 because of its relationship with poor prognosis.

To identify important functions of chr.17q21-24 amplification, Samroc analysis between amplified and nonamplified groups

on chromosome 17q.21 was performed using the corresponding microarray datasets of the 18 Japanese ovarian CCC samples (GSE39204 and GSE55512). The genes that were upregulated in patients with 17q21 amplification (FDR $q < 0.05$) were analyzed using the Database for Annotation, Visualization and Integrated Discovery (DAVID) functional annotation clustering, revealing that mitochondrion-related categories were significantly enriched (enrichment score 4.84, $P < .001$; Figure 1C). Next, overlapping genes between clinical samples and cell lines that showed a positive correlation between amplification and expression on chr.17q21-24 were identified to focus on functionally important genes on chr.17q21-24. Forty-eight genes had r values greater than .4 in both clinical patients and cell lines (Figure 1D, Table S2, and Figure S2A). Among these 48 genes, we focused on *PDK2* because *PDK2* prevents pyruvate from entering the TCA cycle and regulates mitochondrial metabolism. *PDK2* amplification and expression were positively correlated with the IC50 values of cisplatin in 13 CCC cell lines (GSE 29175) (Figure S2B-D). *PDK2* is one of four PDK isoforms, and by using microarray datasets of the 13 ovarian CCC cell lines and 18 ovarian CCC patients, we evaluated the expression of PDK isoforms. In the cell lines, the expression of *PDK1* and *PDK2* was higher than that of *PDK3* and *PDK4* (Figure S2E). In contrast, *PDK2* expression was the second highest following *PDK4* expression in clinical samples (Figure S2F).

TABLE 1 Clinical summary of the immunostaining results in 76 ovarian clear cell carcinoma patients

Parameter	Case (n = 76)	PDK2 expression		P-value
		Low	High	
Age, y				
<60	53	31	22	.6198
≥60	23	15	8	
FIGO stage				
I	55	38	17	.0108
II, III and IV	21	8	13	
Residual tumor				
Optimal	63	39	24	1.0000
Suboptimal	12	7	5	

Note: P -values were calculated with the Fisher's exact test. *PDK2*, pyruvate dehydrogenase kinase 2.

3.2 | Pyruvate dehydrogenase kinase 2 is associated with poor prognosis in ovarian clear cell carcinoma

Of 76 ovarian CCC patients, IHC showed high *PDK2* expression in 46 patients and low *PDK2* expression in 30 patients (Figure 2A and Table 1). *PDK2* mRNA expression was positively correlated with *PDK2* amplification ($r = .43$, $P = .03$; Figure 2B). The IHC score for *PDK2* expression was positively correlated with the *PDK2* CNV value ($r = .35$, $P = .027$; Figure 2C) and mRNA expression ($r = .65$, $P = .0035$) (Figure 2D). High *PDK2* expression was also associated with advanced stage (Table 1). Kaplan-Meier curve and Cox regression analyses showed that patients with high *PDK2* expression, advanced-stage disease and suboptimal surgery had shorter overall survival (OS) (hazard ratio [HR] 3.326 [1.100-8.86], $P = .0326$, HR 15.292 [4.28-54.68], $P < .0001$, HR 3.049 [1.04-8.94], $P = .0421$, respectively; Figure 2E and Table S3) and shorter PFS (HR 2.45 [1.06-5.62], $P = .0352$, HR 26.34 [9.53-72.82], $P < .0001$, HR 5.91 [2.576-13.55], $P < .0001$, respectively; Figure 2F and Table S4) than those with low *PDK2* expression in the univariate analysis. Multivariate analysis revealed that advanced stage was an independent prognostic factor for OS and PFS ($P < .0001$ for both, Tables S3 and S4), and suboptimal surgery was an independent prognostic factor for PFS ($P = .0009$, Table S4). We validated these results using PrognScan (Table S5), which showed the same trends.¹⁶ These results suggest that more aggressive disease occurs in patients with higher expression of *PDK2*.

3.3 | Pyruvate dehydrogenase kinase 2 inhibition has synergistic effects with cisplatin by enhancing apoptosis in vitro

Because *PDK2* amplification is associated with cisplatin resistance in silico, the contribution of *PDK2* to cisplatin resistance was assessed in vitro. We first generated a *PDK2*-silenced cell line, RMG1-sh*PDK2*, using the *PDK2*-expressing ovarian CCC cell line, RMG1, and confirmed the results with RT-PCR and immunoblotting (Figure 3A-upper). The proliferation rate of RMG1-sh*PDK2* cells was the same as that of a control cell line, RMG1-shcontrol. (Figure 3A-lower). Cleaved caspase-3 was analyzed by immunoblotting and immunofluorescence after 24 hours of exposure to cisplatin. In RMG1-sh*PDK2* cells, significantly more cleaved caspase-3 was detected than in RMG1-shcontrol cells at the same concentration

FIGURE 3 Pyruvate dehydrogenase kinase 2 (*PDK2*) inhibition has synergistic effects with cisplatin by enhancing apoptosis in vitro. A and D, quantitative PCR (qPCR), immunoblotting and proliferation curves of RMG1-sh*PDK2* (A) and RMG5-PDK2 (D). B, E, and F, Western blot analysis of cleaved caspase-3 after treatment with cisplatin for 24 h in RMG1-sh*PDK2* (B), RMG5-PDK2 (E), and RMG1-WT (F). C and G, Immunofluorescence staining for cleaved caspase-3 in RMG1-sh*PDK2* cells after treatment with cisplatin for 24 h (C) and RMG1-WT cells with cisplatin + 10 mmol/L DCA for 24 h (G). (magnification: $\times 20$). H and I, Growth inhibition curve of RMG1-sh*PDK2* with cisplatin (H) and RMG1 with cisplatin + 10 mmol/L DCA (I). J-M, Growth inhibition curve of RMG1-sh*PDK2* with cisplatin and in combination with 1 mmol/L NAC for 24 h (J) and pretreatment with 2 mmol/L L-glutathione reduced (GSH) for 1 h before cisplatin (CDDP) for 24 h (L), and the viability at 10 and 20 $\mu\text{mol/L}$ cisplatin with or without 1 mmol/L NAC (K) and 2 mmol/L GSH (M), normalized by viability treated with vehicle. (DCA; sodium dichloroacetate, NAC; N-acetyl-L-cysteine, GSH; L-glutathione reduced, * $P < .05$, ** $P < .01$, *** $P < .001$, Ns, not significant, two-way ANOVA followed by Sidak's multiple comparison test)

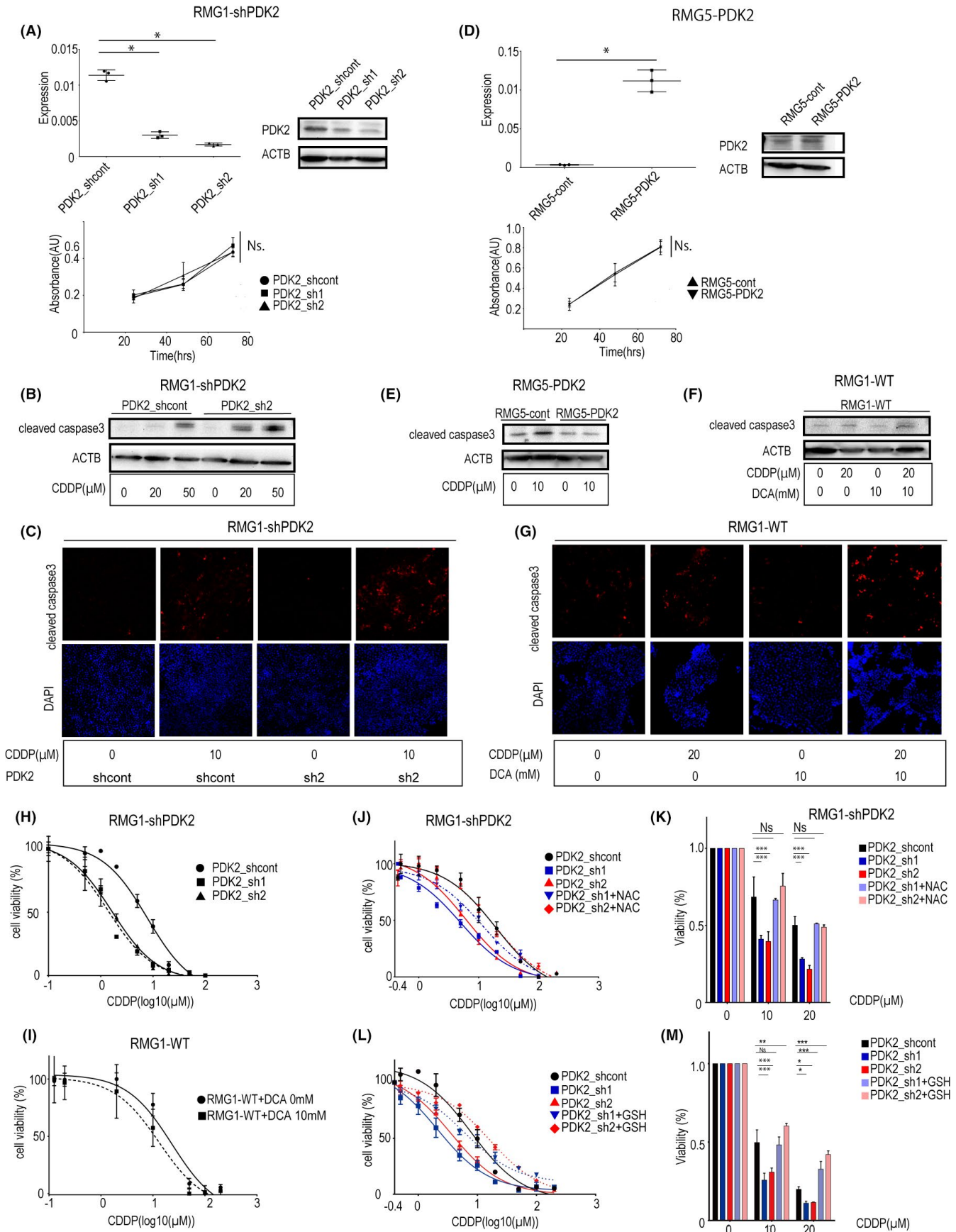


(Figure 3B,C). We also generated a PDK2-overexpressing cell line, RMG5-PDK2 (Figure 3D). In RMG5-PDK2 cells, the production of cleaved caspase-3 was suppressed more than in a control cell line at the same concentration (Figure 3E). DCA, a PDK inhibitor, in combination with cisplatin induced more abundant cleaved caspase-3 in ovarian CCC cells than in cells treated with a control, cisplatin or DCA alone (Figure 3F,G). The IC50 values of RMG1-shPDK2 were 1.365 and 1.648 $\mu\text{mol/L}$ (sh1 and sh2, respectively), whereas the IC50 value was 7.842 $\mu\text{mol/L}$ for RMG1-shcontrol (Figure 3H). DCA also had a synergistic effect with cisplatin (combination index; CI < 1, Figure 3I). These results indicate that high PDK2 expression leads to cisplatin resistance by suppressing apoptosis in vitro.

Next, we assessed the mechanism of cisplatin resistance in PDK2. Inhibition of PDK2 by DCA did not change the expression of CTR1, the CDDP transporter, also known as solute carrier family 31 member 1 (SLC31A1) (Figure S3). To determine the contribution of ROS to cell killing by cisplatin, a viability assay with a combination of cisplatin and an antioxidant reagent, N-acetyl-L-cysteine (NAC), was performed. The addition of 1 mmol/L NAC to cisplatin reduced the production of mitochondrial ROS (Figure S4A) and significantly recovered the viability of RMG1-shPDK2 cells to the same level as RMG1-shcontrol cells (Figure 3J,K), indicating that additional ROS production leads to sensitivity to cisplatin in RMG1-shPDK2 cells. The addition of another antioxidant reagent, GSH, also recovered the viability of RMG1-shPDK2 cells to the same level as RMG1-shcontrol cells compared with RMG1-shPDK2 cells (Figure 3L,M). Again, we confirmed that the addition of GSH to cisplatin reduced the production of mitochondrial ROS (Figure S4B).

3.4 | Suppression of pyruvate dehydrogenase kinase 2 enhances reactive oxygen species production through mitochondrial metabolism

The expression of the PDHE1-alpha subunit phosphorylated at S293 (phospho-pyruvate dehydrogenase [PDH]) in RMG1-shPDK2 cells was confirmed by immunoblotting. Suppression of PDK2 reduced the ratio of phospho-PDH to PDH (Figure S5A). A decreased ratio of phospho-PDH to PDH expression was observed in RMG1 cells treated with DCA (Figure S5B). These findings suggest that PDK2 inhibits PDH function through phosphorylation of PDH.

To clarify the mechanism of the synergistic effect of PDK2 inhibition and cisplatin, the alteration in mitochondrial function induced by PDK2 suppression was investigated by measuring the

oxygen consumption rate (Figure 4A). Suppression of PDK2 led to increased adenosine triphosphate (ATP) production, basal respiration, and maximum respiration (Figure 4B-D). These findings suggest that the suppression of PDK2 induces OXPHOS in mitochondria. In RMG1-shPDK2 cells, administration of 5 $\mu\text{mol/L}$ cisplatin induced a decrease in the spare respiratory capacity and increased proton leak compared to 0 $\mu\text{mol/L}$ cisplatin, suggesting that mitochondrial function was restricted, whereas RMG1-shcontrol cells did not have reduced mitochondrial spare capacity after treatment with 5 $\mu\text{mol/L}$ cisplatin (Figure 4E,F). These results indicate that cisplatin disrupts mitochondrial function due to the activation of OXPHOS induced by suppression of PDK2.

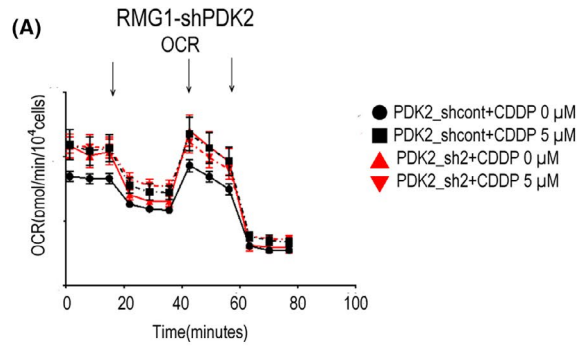
Because suppression of PDK2 leads to increased OXPHOS (Figure 4A), it has been suggested that suppression of PDK2 could produce more ROS in mitochondria. Mitochondrial ROS, as assessed by MitoSOX Red Mitochondrial Superoxide Indicator, showed that significantly more mitochondrial ROS were produced in RMG1-shPDK2 than in RMG1-shcontrol ($P < .001$, Figure 4G and Figure S6A-upper, and B-upper). When cisplatin was administered, significantly more mitochondrial ROS were produced in RMG1-shPDK2 cells than in RMG1-shcontrol cells ($P < .001$, Figure 4G and Figure S6A-upper, and B-upper). When the PDK inhibitor, DCA, was administered with cisplatin, significantly more ROS were detected in RMG1 cells than in RMG1 cells without DCA ($P < .001$, Figure 4H and Figure S6C-upper and D-upper).

Next, mitochondrial membrane potential was assessed by MitoTracker Red-ros. With administration of cisplatin, the mitochondrial membrane potential was diminished in RMG1-shPDK2 cells (Figure 4I and Figure S6A-middle, and B-lower). DCA administered with cisplatin induced a decrease in the mitochondrial membrane potential in RMG1 cells (Figure 4J and Figure S6C-middle, and D-lower). These results suggest that suppression of PDK2 activated mitochondrial OXPHOS and impaired the mitochondrial membrane potential with cisplatin through the production of mitochondrial ROS.

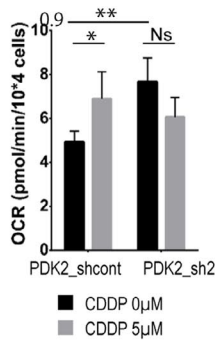
3.5 | Pyruvate dehydrogenase kinase 2 inhibition has a synergistic effect with cisplatin in vivo

Although there was no difference between the tumor growth in RMG1-shcontrol, RMG1-shPDK2, and RMG1-shcontrol cells treated with cisplatin, the tumor growth of RMG1-shPDK2 cells treated with cisplatin was significantly suppressed compared with that of the

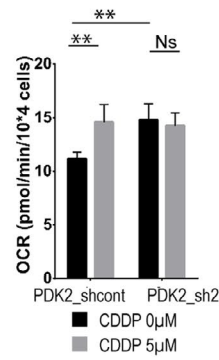
FIGURE 4 Suppression of PDK2 with cisplatin enhances ROS production and reduces mitochondrial function. A, Measurement of OCR in RMG1-shPDK2 control/sh2 cells with or without 5 $\mu\text{mol/L}$ cisplatin, as normalized by cell number. The downward arrows show the injection points for oligomycin (1 $\mu\text{mol/L}$), FCCP (1 $\mu\text{mol/L}$), and rotenone/actinomycin (both 1 $\mu\text{mol/L}$) from left to right. B-F, Quantification of ATP production (B), basal respiration (C), maximal respiration (D), spare respiratory capacity (E), and proton leak (F) in RMG1-shPDK2 control/sh2 cells with or without 5 $\mu\text{mol/L}$ cisplatin. (* $P < .05$, ** $P < .01$, *** $P < .001$; two-way ANOVA followed by Sidak's multiple comparison test). G and H, Representative images of fluorescence for mitoSOX in RMG1-shPDK2 with or without 10 $\mu\text{mol/L}$ cisplatin (G) and RMG1-wild type with or without 20 $\mu\text{mol/L}$ cisplatin + 10 mmol/L DCA (H). (DCA; sodium dichloroacetate), I and J, Representative images of fluorescence for mitoTrackerRed in RMG1-shPDK2 cells with or without 10 $\mu\text{mol/L}$ cisplatin (I) and RMG1-wild type cells with or without 20 $\mu\text{mol/L}$ cisplatin + 10 mmol/L DCA (J). (magnification: G, H, I, and J $\times 20$)



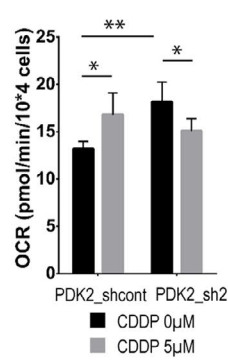
(B) ATP production



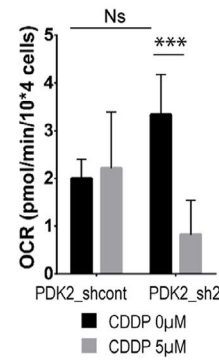
(C) Basal Respiration



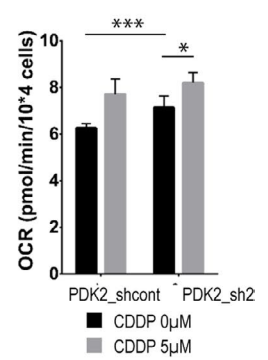
(D) Maximal Respiration



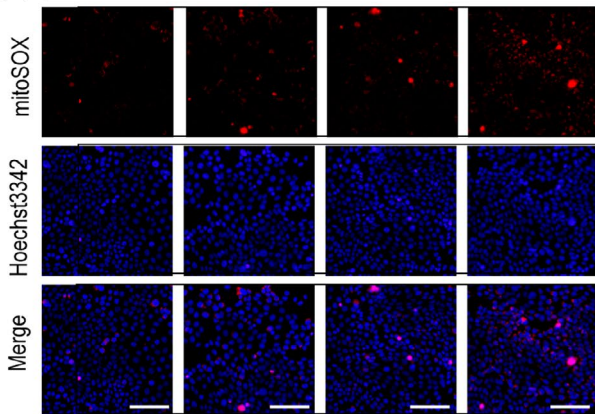
(E) Spare Respiratory Capacity



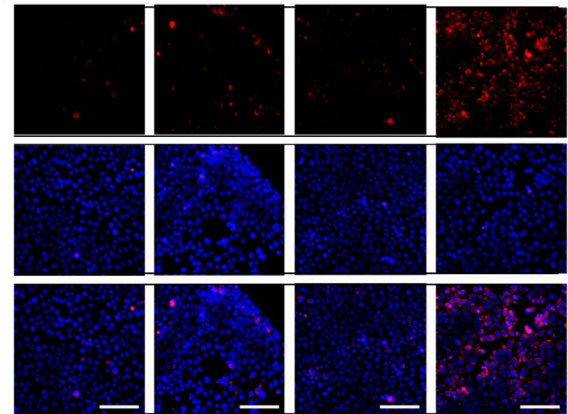
(F) Proton Leak



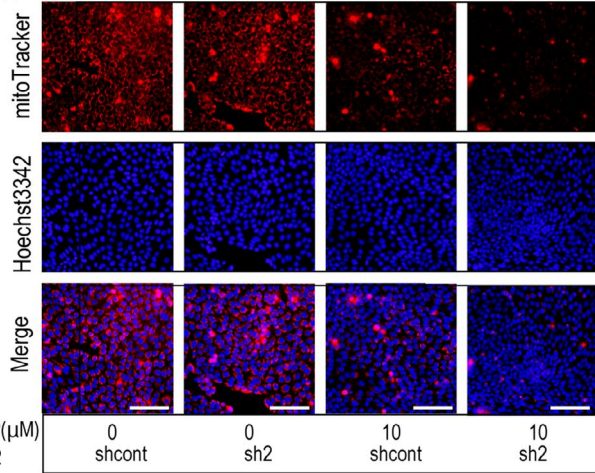
(G) RMG1-shPDK2



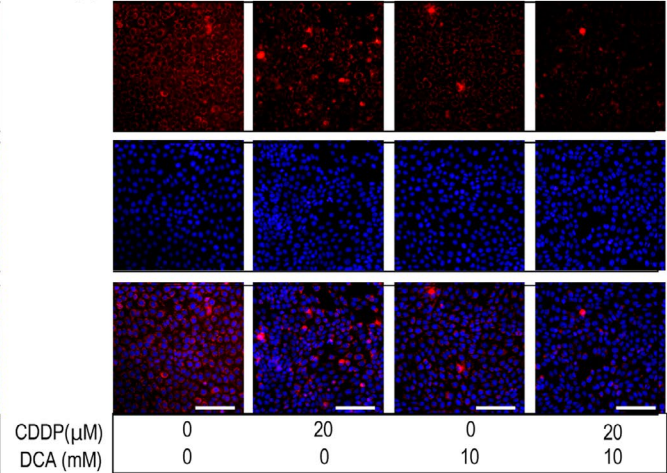
(H) RMG1-WT



(I)



(J)



— 100 μ m

other groups ($P < .01$, Figure 5A,B). Next, tumor growth was assessed using RMG1 subcutaneously inoculated mice administered a control, cisplatin, DCA, or cisplatin and DCA. In the cisplatin and DCA group, tumor growth was significantly suppressed compared with that in the other groups ($P < .01$, Figure 5E,F), although in the cisplatin and DCA alone groups, tumor growth was not significantly suppressed compared with that in the control group. There was no difference in the body weight change among these groups (Figure S7).

A significantly greater number of cells positive for cleaved caspase-3 was detected in the tumors of RMG1-shPDK2 mice treated with cisplatin than in the other mice ($P < .05$, Figure 5C,D). In the TUNEL assay, a significantly greater number of positive cells were identified in the tumors of RMG1-shPDK2 mice treated with cisplatin than in the other mice ($P < .05$, Figure S8A and C). The tumors of RMG1 mice treated with cisplatin and DCA had significantly more cells that were positive for cleaved caspase-3 than RMG1 cells treated with mock, cisplatin or DCA (Figure 5G,H). The TUNEL assay showed that significantly many cells were detected in the tumors of RMG1 mice treated with cisplatin and DCA compared with the others ($P < .05$, Figure S8B,D). These results indicate that suppression of PDK2 enhances the inhibition of tumor growth by cisplatin through apoptosis in vivo.

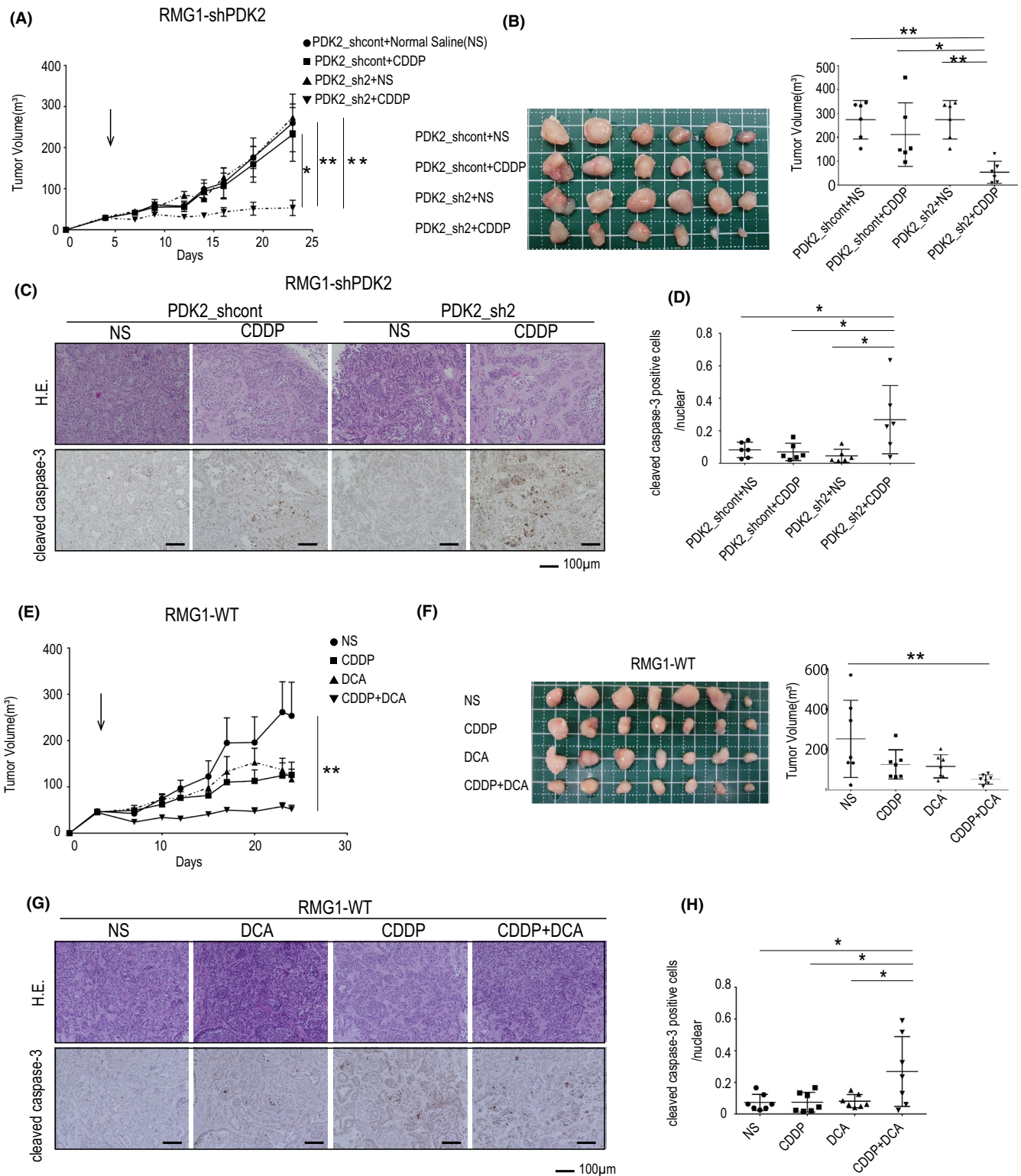
4 | DISCUSSION

One of the significant findings in this study is that chr.17q21-24 amplification is associated with recurrence in ovarian CCC. Several studies have also reported an association between genetic alteration in this region and poor prognosis.^{17,18} Based on these findings, we hypothesized that chr.17q21-24 amplification is related to chemoresistance and metabolism. In this study, the results of in silico analyses suggested that chr.17q21-24 amplification is associated with platinum resistance and mitochondrial metabolism in ovarian CCC. One mechanism of cisplatin resistance is that in the cytoplasm, the interaction between cisplatin and glutathione, metallothionein or mitochondrial proteins, such as voltage-dependent anion channels, results in the depletion of reducing equivalents and/or directly sustains the generation of ROS. ROS can directly trigger mitochondrial outer membrane permeabilization or exacerbate cisplatin-induced DNA damage, thereby playing a dual role in cisplatin cytotoxicity.¹⁹

Another mechanism is reduced intracellular accumulation of cisplatin.¹⁹ The mRNA expression of a major cisplatin transporter, CTR1, was not affected by a PDK2 inhibitor. The other mechanism of cisplatin resistance is increased homologous recombination proficiency. *BRCA1*, *RAD51C*, and *BRIP1* were among 48 candidate genes that showed a positive correlation between amplification and expression on chr.17q21-24 (Table S2). *BRCA1*, *RAD51C*, and *BRIP1* play important roles in homologous recombination, and their genes are located on chr.17q21.31, chr.17q22, and chr.17q23.2, respectively. It has also been reported that *BRCA1*, *RAD51C* or *BRIP1* overexpression induces resistance to cisplatin by enhancing DNA repair.^{20,21} Although our analysis did not identify the homologous recombination proficiency for chemoresistance, this is another possible mechanism for the cisplatin resistance of chr.17q21-24 amplification. DAVID functional annotation clustering indicated that genes of the ubiquitin-proteasome system were also represented among the 48 candidate genes. TP53 mutation is rare in ovarian CCC, although genes functionally inhibiting P53, such as *MDM2 proto-oncogene (MDM2)* and *protein phosphatase, Mg2+/Mn2+ dependent 1D (PPM1D)*, are known to be upregulated.^{22,23} The ubiquitin-proteasome system not only inactivates p53 but also contributes to chemoresistance in some types of cancers.²⁴ An association between 17q21-qter gain and chemoresistance has been reported in acute myelogenous leukemia,²⁵ yet the contribution of 17q21 amplification to platinum resistance and mitochondrial metabolism has not been elucidated, including in ovarian cancer. Therefore, we focused on the ability of ovarian CCC to maintain redox homeostasis in terms of mitochondrial metabolism and further examined the biological mechanism of platinum resistance through exploration of mitochondrial function in ovarian CCC.

The expression of PDK2, which is located on chr.17q21.33, is upregulated according to the amplification in our clinical samples and cell lines. We focused on PDK2 because its amplification is accompanied by high expression. Gene amplification is not always associated with expression level, and amplification, which involves expression dosage, is important. PDK2 is associated with mitochondrial metabolism because it inhibits pyruvate dehydrogenase complex (PDC) by phosphorylation of PDHE1- α on Ser293, which is the gatekeeper of glucose oxidation.¹³ There are four PDK isozymes: PDK1, PDK2, PDK3, and PDK4. Using microarray datasets of the 13 ovarian CCC cell lines and 18 ovarian CCC patients, we evaluated the expression of PDK isoforms. In the cell lines, the expression

FIGURE 5 Pyruvate dehydrogenase kinase 2 (PDK2) inhibition has synergistic effects with cisplatin in vivo. A and B, Growth curve (A), tumor images (B-left), and tumor volume (B-right) of the mouse xenograft models inoculated subcutaneously with RMG1-shcontrol and RMG1-shPDK2 cells treated with NS or cisplatin (5 mg/kg i.p. once a week) ($n = 6$, each group). C, Representative immunostaining image of cleaved caspase-3 and H&E staining of the tumors using RMG1-shcontrol, RMG1-shPDK2, RMG1-shcontrol cells treated with cisplatin, and RMG1-shPDK2 cells treated with cisplatin. D, Quantification of cleaved caspase-3-positive cells normalized to the number of nuclei in the tumors using RMG1-shcontrol, RMG1-shPDK2, RMG1-shcontrol cells treated with cisplatin, and RMG1-shPDK2 cells treated with cisplatin. E and F, Growth curve (E), tumor images (F-left), and tumor volume (F-right) of the mouse xenograft models inoculated subcutaneously with RMG1 administered NS, cisplatin (5 mg/kg i.p. once a week), DCA (59 mg/kg gavage every day), or cisplatin + DCA ($n = 7$, each group). G, Representative immunostaining image of cleaved caspase-3 and H&E staining of the tumors treated with a control, cisplatin, DCA, or cisplatin + DCA. H, Quantification of cleaved caspase-3-positive cells normalized to the number of nuclear cells in the tumors treated with a control, cisplatin, DCA, or cisplatin + DCA. (DCA; sodium dichloroacetate, NS; normal saline, magnification: C and G $\times 20$, * $P < .05$, ** $P < .01$, *** $P < .001$; one-way ANOVA followed by Tukey's multiple comparisons test)



of PDK1 and PDK2 was higher than that of the other isoforms. In contrast, PDK2 expression was the second highest following PDK4 expression in clinical samples. The activity of PDC is changed by reversible phosphorylation, in which phosphorylation of any one of three serine residues (site 1, serine 293; site 2, serine 300; site 3, serine 232) on the alpha subunit of E1 (E1 α) component renders the entire complex inactive. Each PDK exhibits different specificities

for phosphorylation of the E1 α subunit; site 1: PDK2 > PDK4, PDK1 > PDK3, site 2: PDK3 > PDK4, PDK2 > PDK1).¹² Taken together with the results of in silico analyses, we propose that PDK2 plays crucial roles in ovarian CCC. Our data confirmed the mechanism that shows that the ratio of phosphorylation of Ser293 on PDHE1-alpha to total pyruvate dehydrogenase is suppressed by inhibiting PDK2 expression, indicating that PDK2 suppresses the

conversion of pyruvic acid to acetyl coenzyme A, which enters the TCA cycle in mitochondria. Thus, PDK2 can change the production of ROS in the mitochondrial ETC by regulating influx into the TCA cycle. Indeed, increased glycolysis and PDK2 overexpression decrease the production of ROS in mitochondria, thereby inducing resistance to oxidative stress, and are closely linked to cisplatin resistance in head and neck cancer cells; the latter can be overcome by DCA, which is a PDK inhibitor.²⁶ Compared to normal cells, several human cancer cells have high mitochondrial membrane potential and low expression of the K⁺ channel, Kv1.5.²⁷ Therefore, DCA shifts metabolism from glycolysis to glucose oxidation, decreases mitochondrial membrane potential, increases mitochondrial hydrogen peroxide (H₂O₂), and activates Kv channels in cancer cells, inducing apoptosis, decreases in proliferation, and inhibition of tumor growth. In this study, we demonstrated that suppression of PDK2-activated OXPHOS may lead to ETC overload and greater production of ROS in mitochondria. Moreover, we also demonstrated that inhibition of PDK2 coupled with cisplatin treatment significantly reduced the mitochondrial transmembrane potential, thereby inducing apoptosis by increasing mitochondrial ROS generation. The ROS scavenger NAC was found to reduce mitochondrial ROS production and inhibit cell killing by cisplatin. Another ROS scavenger, GSH, also decreased the cell viability by PDK2 knockdown with cisplatin. Rossella et al²⁸ reported that cisplatin exposure induced a mitochondria-dependent ROS response that significantly contributed to cell death by enhancing the cytotoxic effect exerted by nuclear DNA damage. They demonstrated that cisplatin-induced ROS generation occurred as a consequence of its direct effect on mitochondrial DNA, resulting in impaired ETC protein synthesis in cancer cell lines and a yeast model system.²⁸ These results suggest that in ovarian CCC, PDK2 inhibition produces more mitochondrial ROS by activating ETC and that PDK2 inhibition coupled with cisplatin-induced ROS disturbs redox homeostasis, resulting in apoptosis.

Ovarian CCC is characterized by its clear and glycogen-enriched cytoplasm. PDK2 has been reported to be associated with hypoxia-inducible factor-1 α (HIF1A), which is overexpressed in ovarian CCC.^{7,29} Sutendra et al³⁰ showed that mitochondrial activation by inhibiting PDK2 suppresses HIF1A signaling and angiogenesis in cancer. Sun et al³¹ showed that the mitochondrial ND2 mutation contributes to HIF1A accumulation through increased ROS production and upregulation of PDK2, attenuating PDH activity and, thereby, increasing pyruvate, resulting in HIF1A stabilization. HIF-1 transactivates the genes encoding the enzymes required to convert glucose to glycogen, including hexokinase (HK1 or HK2), phosphoglucomutase 1 (PGM1), UDP-glucose pyrophosphorylase (UGP2), glycogen synthase (GYS1), glycogen branching enzyme (GBE1), and the gene encoding protein phosphatase 1 regulatory subunit 3C (PPP1R3C), which activates GYS1 and inhibits liver-type glycogen phosphorylase (PYGL), the enzyme that breaks down glycogen.³² These findings suggest that the metabolic features of ovarian CCC with high PDK2 expression can be related to its morphology.

We also demonstrated, using clinical data, that high expression of PDK2 is associated with recurrence and advanced-stage disease

and, using ovarian CCC cell lines, with chemoresistance. In ovarian cancer, advanced-stage disease is a risk factor for recurrence.³³ Cancer recurrence after treatment is reported to be associated with tumor progression, acquired drug resistance, cancer stemness, and escape from immune surveillance.³⁴ Mitochondria play crucial roles in these processes.³⁵ We demonstrated that PDK2 expression influences mitochondrial metabolism, mitochondrial function, and drug resistance *in vitro* and *in vivo*. These findings suggest that PDK2 can influence multiple processes during cancer progression, including recurrence, through chemoresistance in ovarian CCC. Because ovarian CCC shows frequent mutations in many genes,^{4,36} several oncogenic pathways are activated synchronously in ovarian CCC. Therefore, molecular targeted therapy, such as the use of mTOR inhibitors, against ovarian CCC has failed to develop. In this way, although CCC exhibits malignant behaviors, including chemoresistance, no effective therapeutic agents have been developed. Targeting mitochondrial metabolism is a promising strategy because mitochondrial metabolism fulfills a crucial role in ovarian CCC.

There are several limitations of our study. First, we did not evaluate interactions between multiple genes on chr.17q21-24. Arm-level chromosomal deletion and amplification are common in cancer.³⁷ Cai et al stated that concomitant loss of multiple genes triggered by large-scale deletions could create phenotypes that fundamentally differed from those arising from the loss of a single tumor-suppressor gene and should be considered and studied as distinct mutational events. To overcome this problem, they modeled the loss of heterozygosity in chromosome 8p using transcription activator-like effector nuclease (TALEN)-based genomic engineering.³⁸ Unfortunately, we could not evaluate the effect of chr.17q21-24 amplifications because there are no biomolecular models that can induce large-scale amplifications. Second, the intratumor heterogeneity of cancer metabolism was not evaluated. Brooks et al presented a novel approach incorporating functional imaging with multiregional gene expression profiling to facilitate the assessment of intratumor heterogeneity. They demonstrated that different subtypes of the same tumor had different glucose metabolism.³⁹ Third, we showed that high PDK2 expression is associated with advanced disease stages. Our clinical cases, however, included limited numbers of advanced cases.

In summary, our work suggests that in ovarian CCC: (a) chr.17q21-24 amplification is associated with recurrence and platinum resistance; (b) high PDK2 expression is a prognostic factor; and (c) PDK2 inhibition with cisplatin upregulates mitochondrial ROS, which disturbs redox homeostasis and leads to apoptosis and inhibition of tumor growth *in vitro* and *in vivo*. This study provides new insight for understanding drug resistance in ovarian CCC in terms of mitochondrial metabolism and redox homeostasis.

ACKNOWLEDGMENTS

KAKENHI, Grant-in-Aid for Scientific Research, #20378772

DISCLOSURE

The authors declare no potential conflicts of interest.

ORCID

Ken Yamaguchi  <https://orcid.org/0000-0002-7669-1405>

Ryusuke Murakami  <https://orcid.org/0000-0001-5007-5674>

Junzo Hamanishi  <https://orcid.org/0000-0002-7750-0623>

REFERENCES

- Siegel R, Ma J, Zou Z, Jemal A. Cancer statistics, 2014. *CA Cancer J Clin.* 2014;64:9-29.
- Yahata T, Banzai C, Tanaka K, Registry NGC. Histology-specific long-term trends in the incidence of ovarian cancer and borderline tumor in Japanese females: a population-based study from 1983 to 2007 in Niigata. *J Obstet Gynaecol Res.* 2012;38:645-650.
- Oliver KE, Brady WE, Birrer M, et al. An evaluation of progression free survival and overall survival of ovarian cancer patients with clear cell carcinoma versus serous carcinoma treated with platinum therapy: an NRG Oncology/Gynecologic Oncology Group experience. *Gynecol Oncol.* 2017;147:243-249.
- Wang YK, Bashashati A, Anglesio MS, et al. Genomic consequences of aberrant DNA repair mechanisms stratify ovarian cancer histotypes. *Nat Genet.* 2017;49:856-865.
- Liu J, Matulonis UA. New strategies in ovarian cancer: translating the molecular complexity of ovarian cancer into treatment advances. *Clin Cancer Res.* 2014;20:5150-5156.
- Yamaguchi K, Mandai M, Toyokuni S, et al. Contents of endometriotic cysts, especially the high concentration of free iron, are a possible cause of carcinogenesis in the cysts through the iron-induced persistent oxidative stress. *Clin Cancer Res.* 2008;14:32-40.
- Yamaguchi K, Mandai M, Oura T, et al. Identification of an ovarian clear cell carcinoma gene signature that reflects inherent disease biology and the carcinogenic processes. *Oncogene.* 2010;29:1741-1752.
- Amano Y, Mandai M, Yamaguchi K, et al. Metabolic alterations caused by HNF1 β expression in ovarian clear cell carcinoma contribute to cell survival. *Oncotarget.* 2015;6:26002-26017.
- Cottet-Rousselle C, Ronot X, Leverve X, Mayol JF. Cytometric assessment of mitochondria using fluorescent probes. *Cytometry A.* 2011;79:405-425.
- Porporato P, Payen VL, Pérez-Escuredo J, et al. A mitochondrial switch promotes tumor metastasis. *Cell Rep.* 2014;8:754-766.
- Yang Y, Karakhanova S, Hartwig W, et al. Mitochondria and mitochondrial ROS in cancer: novel targets for anticancer therapy. *J Cell Physiol.* 2016;231:2570-2581.
- Saunier E, Benelli C, Bortoli S. The pyruvate dehydrogenase complex in cancer: an old metabolic gatekeeper regulated by new pathways and pharmacological agents. *Int J Cancer.* 2016;138:809-817.
- Stacpoole PW. Therapeutic targeting of the pyruvate dehydrogenase complex/pyruvate dehydrogenase kinase (PDC/PDK) axis in cancer. *J Natl Cancer Inst.* 2017;109. <https://doi.org/10.1093/jnci/djx071>
- Abiko K, Mandai M, Hamanishi J, et al. PD-L1 on tumor cells is induced in ascites and promotes peritoneal dissemination of ovarian cancer through CTL dysfunction. *Clin Cancer Res.* 2013;19:1363-1374.
- Abiko K, Matsumura N, Hamanishi J, et al. IFN- γ from lymphocytes induces PD-L1 expression and promotes progression of ovarian cancer. *Br J Cancer.* 2015;112:1501-1509.
- Mizuno H, Kitada K, Nakai K, Sarai A. PrognoScan: a new database for meta-analysis of the prognostic value of genes. *BMC Med Genomics.* 2009;2:18.
- Suehiro Y, Sakamoto M, Umayahara K, et al. Genetic aberrations detected by comparative genomic hybridization in ovarian clear cell adenocarcinomas. *Oncology.* 2000;59:50-56.
- Hirasawa A, Saito-Ohara F, Inoue J, et al. Association of 17q21-q24 gain in ovarian clear cell adenocarcinomas with poor prognosis and identification of PPM1D and APPBP2 as likely amplification targets. *Clin Cancer Res.* 2003;9:1995-2004.
- Galluzzi L, Senovilla L, Vitale I, et al. Molecular mechanisms of cisplatin resistance. *Oncogene.* 2012;31:1869-1883.
- Chen X, Qian D, Cheng J, et al. High expression of Rad51c predicts poor prognostic outcome and induces cell resistance to cisplatin and radiation in non-small cell lung cancer. *Tumour Biol.* 2016;37:13489-13498.
- Liu YU, Li H, Zhang R, et al. Overexpression of the BRIP1 ameliorates chemosensitivity to cisplatin by inhibiting Rac1 GTPase activity in cervical carcinoma HeLa cells. *Gene.* 2016;578:85-91.
- Crane EK, Kwan S-Y, Izaguirre DI, et al. Nutlin-3a: a potential therapeutic opportunity for TP53 wild-type ovarian carcinomas. *PLoS One.* 2015;10:e0135101.
- Fiscella M, Zhang H, Fan S, et al. Wip1, a novel human protein phosphatase that is induced in response to ionizing radiation in a p53-dependent manner. *Proc Natl Acad Sci USA.* 1997;94:6048-6053.
- Konac E, Varol N, Kiliccioglu I, Bilen CY. Synergistic effects of cisplatin and proteasome inhibitor bortezomib on human bladder cancer cells. *Oncol Lett.* 2015;10:560-564.
- Morerio C, Russo I, Rosanda C, et al. 17q21-qter trisomy is an indicator of poor prognosis in acute myelogenous leukemia. *Cancer Genet Cytogenet.* 2001;124:12-15.
- Roh JL, Park JY, Kim EH, Jang HJ, Kwon M. Activation of mitochondrial oxidation by PDK2 inhibition reverses cisplatin resistance in head and neck cancer. *Cancer Lett.* 2016;371:20-29.
- Bonnet S, Archer SL, Allalunis-Turner J, et al. A mitochondria-K⁺ channel axis is suppressed in cancer and its normalization promotes apoptosis and inhibits cancer growth. *Cancer Cell.* 2007;11:37-51.
- Marullo R, Werner E, Degtyareva N, et al. Cisplatin induces a mitochondrial-ROS response that contributes to cytotoxicity depending on mitochondrial redox status and bioenergetic functions. *PLoS One.* 2013;8:e81162.
- Lee S, Garner EI, Welch WR, Berkowitz RS, Mok SC. Overexpression of hypoxia-inducible factor 1 alpha in ovarian clear cell carcinoma. *Gynecol Oncol.* 2007;106:311-317.
- Sutendra G, Dromparis P, Kinnaird A, et al. Mitochondrial activation by inhibition of PDKII suppresses HIF1a signaling and angiogenesis in cancer. *Oncogene.* 2013;32:1638-1650.
- Sun W, Zhou S, Chang SS, McFate T, Verma A, Califano JA. Mitochondrial mutations contribute to HIF1alpha accumulation via increased reactive oxygen species and up-regulated pyruvate dehydrogenase kinase 2 in head and neck squamous cell carcinoma. *Clin Cancer Res.* 2009;15:476-484.
- Semenza GL. HIF-1 mediates metabolic responses to intratumoral hypoxia and oncogenic mutations. *J Clin Invest.* 2013;123:3664-3671.
- Heintz A, Odicino F, Maisonneuve P, et al. Carcinoma of the ovary. FIGO 26th annual report on the results of treatment in gynecological cancer. *Int J Gynaecol Obstet.* 2006;95(Suppl 1):S161-S192.
- Páez D, Labonte MJ, Bohanes P, et al. Cancer dormancy: a model of early dissemination and late cancer recurrence. *Clin Cancer Res.* 2012;18:645-653.
- Porporato PE, Filigheddu N, Pedro JMB, Kroemer G, Galluzzi L. Mitochondrial metabolism and cancer. *Cell Res.* 2018;28:265-280.
- Huang RY, Chen GB, Matsumura N, et al. Histotype-specific copy-number alterations in ovarian cancer. *BMC Med Genomics.* 2012;5:47.
- Beroukhi R, Mermel CH, Porter D, et al. The landscape of somatic copy-number alteration across human cancers. *Nature.* 2010;463:899-905.
- Cai Y, Crowther J, Pastor T, et al. Loss of chromosome 8p governs tumor progression and drug response by altering lipid metabolism. *Cancer Cell.* 2016;29:751-766.

39. Brooks SA, Khandani AH, Fielding JR, et al. Alternate metabolic programs define regional variation of relevant biological features in renal cell carcinoma progression. *Clin Cancer Res.* 2016;22:2950-2959.

SUPPORTING INFORMATION

Additional supporting information may be found online in the Supporting Information section.

How to cite this article: Kitamura S, Yamaguchi K, Murakami R, et al. PDK2 leads to cisplatin resistance through suppression of mitochondrial function in ovarian clear cell carcinoma. *Cancer Sci.* 2021;112:4627-4640. <https://doi.org/10.1111/cas.15125>